Hindawi
Advances in Civil Engineering
Volume 2020, Article ID 6149452, 11 pages
https://doi.org/10.1155/2020/6149452

Research Article

Blasting-Induced Vibration Response of the Transition Section in a Branching-Out Tunnel and Vibration Control Measures

Feng Cao,[1] Sheng Zhang ,[2,3] and Tonghua Ling[4]

[1]*Hunan Provincial Communications Planning, Survey and Design Institute Company Limited, Changsha 410200, China*
[2]*School of Civil Engineering, Hunan City University, Yiyang 413000, China*
[3]*Department of Mechanical Engineering, University of Houston, Houston 77204, USA*
[4]*School of Civil Engineering, Changsha University of Science & Technology, Changsha 410114, China*

Correspondence should be addressed to Sheng Zhang; zhangsheng0403311@163.com

Received 20 February 2020; Revised 2 June 2020; Accepted 4 July 2020; Published 28 July 2020

Academic Editor: Emanuele Brunesi

Blasting-induced vibration during the excavation of transition section in a branching-out tunnel causes damage and hence affects the safety and stability of the supporting structure and surrounding rock. To examine the effects of excavation and blasting of the transition section in the posterior tunnel on the supporting structures of the anterior tunnel, the influences of the blasting-induced vibration in the posterior tunnel on the anterior tunnel were analyzed under different surrounding rock levels, excavation techniques, distances from explosive source, and net spans. This method was performed by combining numerical simulation with blasting-induced vibration monitoring according to the construction characteristics of the transition section in a branching-out tunnel of a highway. A control technique was investigated to assure the safety and stability of the anterior tunnel during the excavation and blasting of the posterior tunnel. Results demonstrate that (1) the vibration velocity peak behind the blasting excavation surface of the tunnel is higher than that in front. These results suggest paying much attention in monitoring vibration velocity within 10 m behind the excavation surface. (2) The blasting-induced vibration velocity peak on the spandrel at the side that faces the blasting in the anterior tunnel is 2.0–2.5 times than that at the side behind the blasting. Moreover, the blasting-induced vibration velocity peak on the haunch at the side that faces the blasting in the anterior tunnel is 6-7 times than that at the side behind the blasting. (3) Instead of the full-face excavation method, the use of center cross diagram (CRD) technique or side wall pilot tunnel method is suggested for the excavation of surrounding rocks of IV-level, V-level, and III-level with a net span smaller than 3 m. (4) Vibration control measures, such as double wedge-shaped cut blasting and floor blast-hole staged detonation, were adopted by designing and optimizing blasting parameters (e.g., total explosives, maximal segment explosive quantity, detonation order, and detonation interval) in posterior tunnel. According to the test, the blasting-induced vibration velocity peak, which is monitored in the anterior tunnel, can be controlled within 10 cm/s to assure the safety and stability of the supporting structure and surrounding rocks of the tunnel.

1. Introduction

Branching-out tunnel, as a novel structural form, attracts increasing attention with the continuous development of high-level highway planning and construction in recent years and the limitations that are due to considerations of land resource utilization and low engineering cost caused by the terrain and construction site [1–3]. The branching-out tunnel is composed of three parts, namely, the large-span, multiarch, and small net span sections. The branching-out tunnel has promising application prospects in difficult highway construction and in transition project of bridges and tunnels because it exhibits the engineering characteristics of large-span multiarch tunnel and neighborhood tunnel [4–6]. However, the distance between the two holes changes continuously, and the stress structures in the transition section become complicated because the blasting excavation of the posterior tunnel in the transition section of the branching-out tunnel can influence the stability of the supporting structure of the anterior tunnel, thereby further

changing the stress state and mechanical behavior of the supporting structure in the tunnel, and even local collapse or overall instability of the supporting structure [7, 8]. These factors cause certain restraints against efficiency of construction and the engineering quality of the tunnel. Therefore, studying the influences of posterior tunnel construction on the stability of the anterior tunnel in the transition section of branching-out tunnel has important practical significance [9, 10].

With respect to the selection of tunnel construction schemes, the drilling and blasting method is a practical technique for underground projects in traffic tunnel, municipal-service tunnel, hydraulic tunnel, and mine tunnel because of its lower operation cost, stronger adaptation, and simpler construction technique compared with tunnel boring machine and shield driving methods [11–13]. Nevertheless, partial energies generated by blast-hole explosion are used to break rocks, whereas the highest energy is transformed into blast, stress, and seismic waves to propagate and connect microdefects on supporting structures and rock masses, thereby decreasing the bearing capacities of the supporting structures and rock masses [14–16]. Abundant field tests and numerical simulation studies on the propagation of blasting-induced vibration in tunnel and its influences on supporting structures and rock masses have been conducted to minimize blasting-related damage to the supporting structures and rock masses [17–19]. However, studies on the attenuation laws of blasting-induced vibration in a branching-out tunnel are limited. In fact, the transition section has become the key part in the blasting excavation of a branching-out tunnel because of the great changes in chamber shapes and supporting structural forms in the transition section of a branching-out tunnel. Therefore, performing numerical simulation and field monitoring test on blasting-induced vibration response features of the transition section of a branching-out tunnel is crucial.

This study combined the engineering characteristics of transition section of a branching-out tunnel to optimize the design of the tunnel blasting scheme and verified and analyzed the blasting scheme by using the measurement data of blasting-induced vibration. Subsequently, the blasting-induced vibration response features of the transition section of a branching-out tunnel under different buried depths, surrounding rock levels, excavation technique, shared rock thicknesses, and net spans were carried out by using a finite element numerical simulation analysis. Finally, some blasting-induced vibration control measures were proposed. This study realized safety and stability during the controlled blasting construction of the transition section of a branching-out tunnel.

2. Project Overview

A highway tunnel adopts the branching-out tunnel and is located in karst middle and low mountainous areas. A great topographic relief along the highway is observed, and the ground elevation ranges between 427.06 and 640.27 m. The maximum buried depth is 185 m. The branching-out section of the tunnel is 138.5 m long and is divided into three sections, namely, large-span, multiarch, and small net span sections. The plan view of the branching-out tunnel is shown in Figure 1, and the profile view of 1–1 is shown in Figure 2. The tunnel transition section is located 20 m in front and rear of the interface between the sandwich multiarch tunnel and the neighborhood tunnel. The characteristics of the transition section of the branching-out tunnel are mainly manifested as the constantly changing width of the sandwich wall, the abrupt cross-sectional shape of the transition section, and the stress concentration. From the geological situation, the surrounding rock of the tunnel is composed of slightly weathered limestone with developed dissolution fissures and relatively broken rock masses. The minimum net span between two adjacent tunnels is 1 m, and the minimum buried depth is only 3 m. The short net span, small buried depth, complicated structural stresses, and soft surrounding rocks in the tunnel bring extremely difficulties to blasting excavation.

3. Design and Verification of Blasting Parameters

3.1. Design of Tunnel Blasting Parameters. According to relevant rules in Safety Regulations for Blasting (GB6722-2014), the critical value of safe particle vibration velocity is 10–20 cm/s [20–22]. Considering the structural uniqueness of the transition section in a branching-out tunnel, the safety critical value of blasting-induced vibration velocity was determined as 10 cm/s. In the blasting design, the net span of the transition section was 2-3 m. The buried depth and surrounding rock level were set 25-35 m and V-level, respectively. The CRD method was applied to excavate rock mass. The CRD method in the posterior tunnel and blast-hole layout in the upper bench left Zone I are shown in Figure 3.

Given that the vibration caused by cut-hole explosion on no-free face is the maximum, the blasting parameters in the upper bench left Zone I of the posterior tunnel were going to be optimized. The optimized blasting design parameters are shown in Table 1, and the blast-hole layout is shown in Figure 3. Double wedge-shaped cut blasting was applied to decrease single cut-hole blasting-induced vibration. Superposition of blasting-induced vibration waves is avoided, and the blasting-induced vibration velocity is decreased by shortening the footage driving cycle, decreasing maximal segment explosive quantity, and setting skip detonators to extend the interval time.

3.2. Verification Analysis of Blasting-Induced Vibration Data. Blasting-induced vibration in the anterior tunnel will be monitored to investigate the influences of posterior tunnel blasting on the vibration of the anterior tunnel. Blasting-induced vibration monitoring points on the section of the anterior tunnel were mainly set at the spandrel, haunch, and arch foot on the side facing with detonation. Monitoring points were set symmetrically on the advancing and retreating directions around the axial line along the

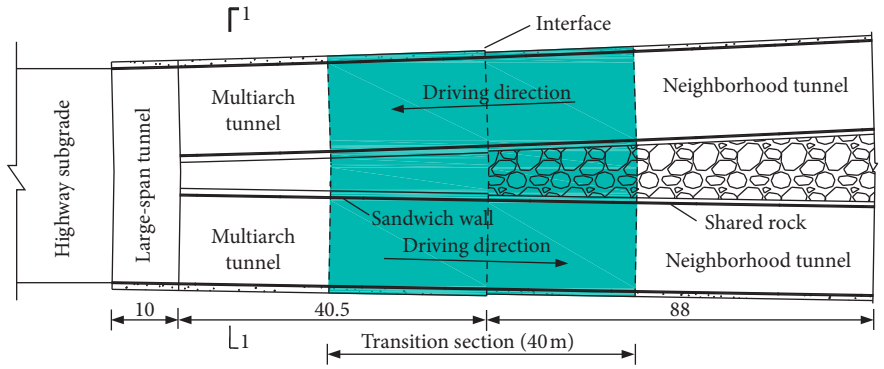

Figure 1: Plan view of the transition section of the branching-out tunnel (unit: m).

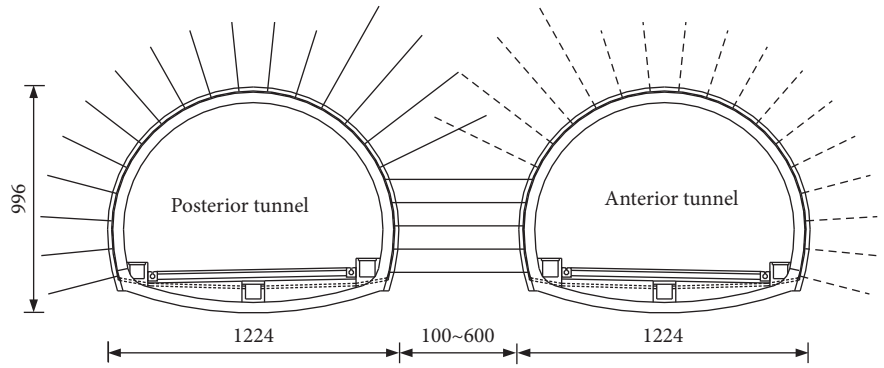

Figure 2: Profile view of 1–1 (unit: cm).

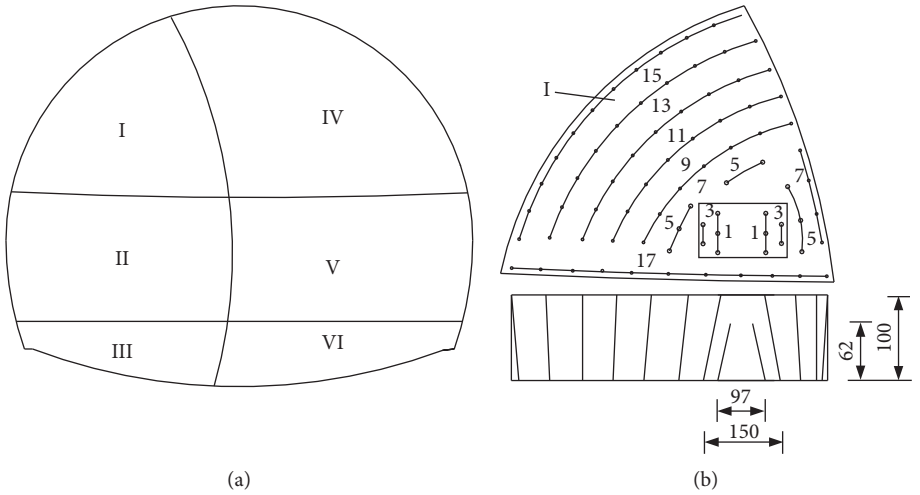

Figure 3: (a) CRD method and (b) blast-hole layout (unit: mm) in the posterior tunnel.

explosive excavation surface. The space between two monitoring points was set as 5 m, and five sections were involved. Three monitoring points were set on each section, thus setting 15 monitoring points. The specific layouts of monitoring points are shown in Figure 4.

Blasting-induced vibration was monitored by using a TC-4850 intelligent vibration monitor. The TC-4850 intelligent vibration monitor had a triaxial vibration velocity sensor. A statistical analysis on monitoring results at different points on haunch, spandrel, and arch foot of the side facing with detonation was carried out. Results are shown in Table 2.

Table 2 shows that radial vibration velocities at all monitoring points are higher than the tangential and vertical vibration velocities. The blasting-induced vibration velocity at the spandrel is higher than those at the haunch and arch foot, and the maximum vibration velocity peak is at the 3# spandrel, which amounts to 8.36 cm/s or is smaller than the critical value of safe particle vibration velocity (10 cm/s). This result reflects that the blasting-induced vibration is controlled.

Table 1: Optimized blasting design parameters.

Sections	Type of holes	Hole depth (m)	Number of holes	Single-hole explosive quantity (kg)	Maximal segment explosive quantity (kg)
1	Cut-hole	1.3	6	0.35	2.10
3	Cut-hole	1.3	4	0.30	1.20
5	Auxiliary hole	1.0	8	0.20	1.60
7	Auxiliary hole	1.0	11	0.20	2.20
9	Auxiliary hole	1.0	8	0.20	1.60
11	Auxiliary hole	1.0	9	0.20	1.80
13	Auxiliary hole	1.0	10	0.15	1.50
15	Periphery hole	1.0	12	0.15	1.80
17	Floor hole	1.2	11	0.25	2.75
Total			79		16.55

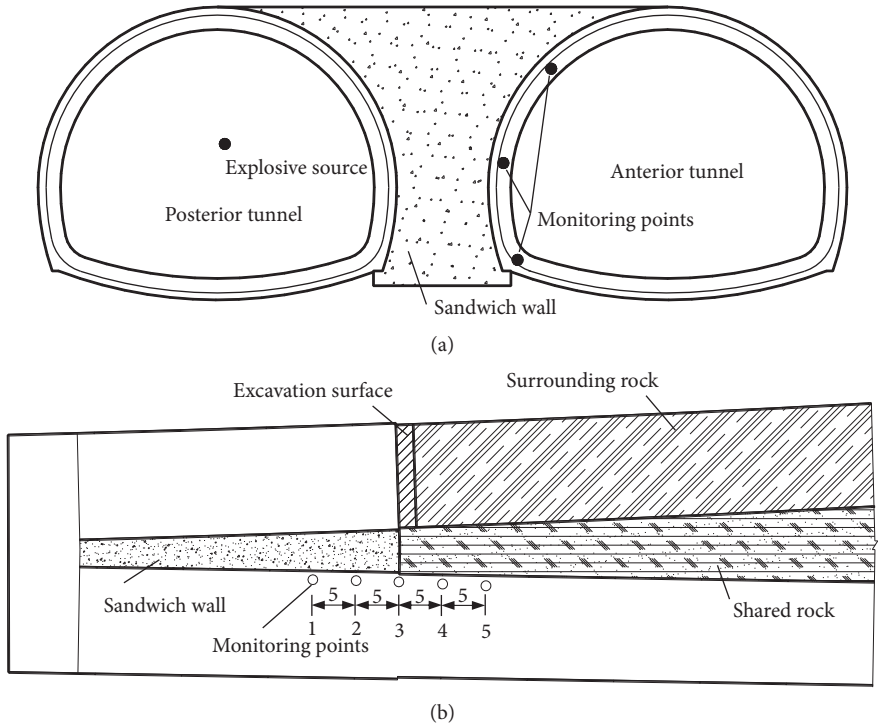

Figure 4: Layouts of vibration velocity monitoring points: (a) sectional layout; (b) plane layout (unit: m).

4. Numerical Verification

4.1. Introduction of LS-DYAN. LS-DYAN is finite element numerical calculation software for geometrical nonlinearity and material nonlinearity. It is suitable for analyzing structural nonlinear impact dynamic problems, such as explosions and structural collisions. Lagrange is the main algorithm used, and ALE and Euler algorithms are also included. The main functions of the LS-DYAN program are to display solutions and structural analysis. It also contains different element libraries, including thin and thick shell elements, beam elements, and other two-dimensional and three-dimensional solid elements. Various types of elements can use multiple algorithms. They also have large strain, displacement, and rotation performance, which can meet the needs of finite element meshing of various solid structures.

The explicit dynamic analysis of ANSYS/LS-DYNA includes three basic operations, namely, preprocessing, solving, and postprocessing. In the preprocessing stage, this article mainly uses ANSYS/LS-DYNA software. The workflow can be described as follows: specify the element type; establish a geometric model; divide the mesh; form a finite element model; define the contact surface, construction load, and boundary conditions; and import the information into the K file. Then, submit the K file to the LS-DYNA solver for result. Finally, postprocessors POST1 and POST26 of ANSYS are used to visualize the calculation results.

4.2. Calculation Model and Parameters. Some research results have demonstrated that the net width of the tunnel is an evaluation index of difficulties in vibration-controlled

Table 2: Monitoring data of blasting-induced vibration at different points.

Monitoring points	Position of monitoring points	Maximal segment explosive quantity (kg)	Distance from explosive sources (m)	Peak velocity (cm/s)		
				Radial	Tangential	Vertical
1	Haunch	2.75	17.2	1.61	1.45	1.44
	Spandrel	2.75	17.9	2.23	2.04	2.02
	Arch foot	2.75	18.6	0.91	0.96	1.02
2	Haunch	2.75	14.1	3.07	2.91	2.88
	Spandrel	2.75	14.4	4.32	4.10	4.08
	Arch foot	2.75	15.9	2.13	2.06	2.00
3	Haunch	2.75	11.9	8.01	7.92	5.05
	Spandrel	2.75	12.5	8.36	7.91	7.21
	Arch foot	2.75	14.2	4.54	4.39	4.34
4	Haunch	2.75	12.9	3.42	3.27	3.34
	Spandrel	2.75	13.5	3.67	3.43	3.46
	Arch foot	2.75	15.1	2.07	1.95	1.85
5	Haunch	2.75	15.6	1.98	1.80	1.13
	Spandrel	2.75	16.2	2.50	1.79	1.11
	Arch foot	2.75	17.4	0.86	0.76	0.75

blasting excavation of the posterior tunnel [23, 24]. Given the small net width of the tunnel, the blasting construction of the posterior tunnel can influence the stability of the surrounding rock and supporting structure in the anterior tunnel. In this branching-out tunnel, the transition section with a net span of 1–6 m is used as the analysis region. According to practical field situation, a three-dimensional model was constructed by using the ANSYS/LS-DYNA explicit finite element program to investigate the influence features of blasting-induced vibration in posterior tunnel of the transition section on the supporting structures of the anterior tunnel.

This calculation applied the expanded boundary ranges to reduce the influences of boundary effects. The calculation size of the constructed model was both 75 m at the left and right boundaries. The upper boundary was extended to the surface, and the lower boundary was set to 40 m. The longitudinal length of the tunnel was 100 m. An X-directional displacement constraint was applied on the right and left sides of the model, and a Y-directional displacement constraint was applied on the bottom of the model. The top of the model used a free boundary. The front and back surfaces of the model applied a Z-directional displacement constraint. Nearly all positions of the model were applied with nonreflecting boundaries, except for the top surface of the model. These boundary conditions can avoid the influences of stress wave reflection on the calculation results of the model.

In this numerical calculation model, the explosive corresponds to a continuous coupled charge structure and is set at the center of the charge for detonating; SOLID_164 elements are used for explosives, rock and soil bodies, and concrete. The model is divided by a solid grid, and displacement constraints and nonreflective boundary conditions are carried out on the infinite area and explosive boundary surface that extends outside the rock body. The fluid-solid coupling ALE algorithms are used between the rock and soil bodies and the explosives and concrete. For the explosive, ALE algorithm is used to control the rheology of the unit. The rock, soil, and pipeline are controlled by using the Lagrange algorithm to solve the problem and to reduce the result error caused by the large deformation in the solution calculation. The calculation model is shown in Figure 5. The model adopts the hexahedral mapping grid division unit with high unit order, and the grid division has a total of 213,226 solid units and 221,598 nodes.

According to relevant literature review, the vibration strength caused by blasting in cut-holes is stronger than those of auxiliary and surrounding holes during tunnel blasting [25, 26]. This study focused on the dynamic analysis of blasting in cut-holes. The concentrated charging mode does not affect the studies regarding the influencing laws of vibration waves on the supporting structure of the tunnel. For the convenience of calculation, the cut-hole was simulated by using the concentrated charging mode, and the cut-holes in the same section were simplified into a blasting hole, which was at the low right position of the upper step on the left of the posterior tunnel. The explosion process was simulated by Jones–Wilkens–Lee (JWL) state equation. Pressure in the explosive unit after detonation was calculated from the state equation and was expressed as

$$P_{\text{eos}} = A\left(1 - \frac{\omega}{R_1 V}\right)e^{-R_1 V} + B\left(1 - \frac{\omega}{R_2 V}\right)e^{-R_2 V} + \frac{\omega E_0}{V}, \tag{1}$$

where A, B, R_1, R_2, and ω are constants of the state equation. V is the relative volume, and E_0 is the initial internal energy density.

Pressure in a unit is

$$P = F \times P_{\text{eos}}, \tag{2}$$

where F is the combustion reaction rate of unit.

Explosive was simulated by the MAT_HIGH_EXPLOSIVE_BURN model. The state equation of the explosive was defined by EOS_JWL. Parameters of the applied explosive materials and state equation are shown in Table 3.

According to field investigation, the surrounding rocks in the tunnel include clay and weak weathered limestone

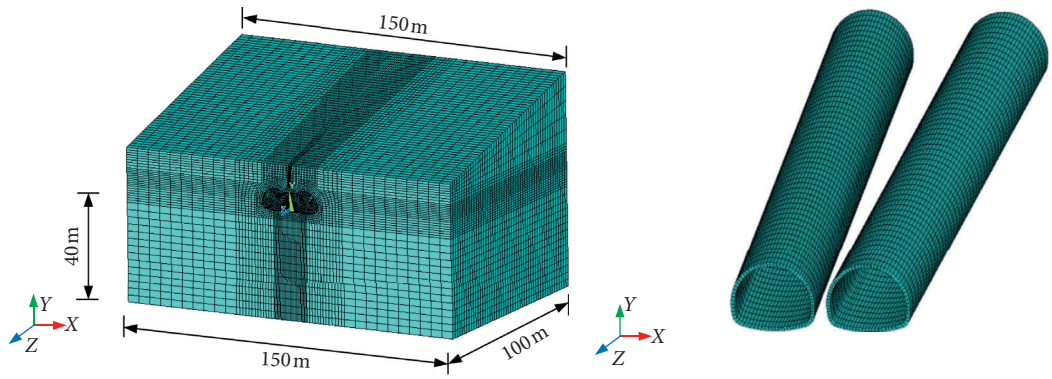

Figure 5: Calculation model and meshing: (a) overall calculation model; (b) tunnel lining model.

Table 3: Parameters of explosive materials.

Density (g/cm^3)	Detonation velocity (m/s)	A (GPa)	B (GPa)	R_1	R_2	ω	E_0 (GPa)
1.1	4200	5.24×10^4	76.9	4.2	1	0.3	8.5

with small thickness on the roof. The primary lining is C20 shotcrete and the secondary lining is C25 concrete. The reinforcement area of rock bolts is estimated according to the Dulacska formula [27]:

$$c_0' = c_0 + \frac{\pi D^2 \sigma_s \left(1/2 + \varphi_0/180^\circ\right)\sin\left(45^\circ + \varphi_0/2\right)}{4\sqrt{3}S_a S_c}, \quad (3)$$

where c_0' is the equivalent cohesion of rock bolts reinforcement area, kPa; c_0 is the initial cohesion of surrounding rock, kPa; φ_0 is the initial internal friction angle of surrounding rock, °; D is the diameter of rock bolts, mm; σ_s is the tensile strength of rock bolts, kPa; S_a is the longitudinal spacing of rock bolts along the tunnel, m; S_c is the annular spacing of rock bolts, m.

The strength of the steel arch is converted to concrete by an equivalent method, and the following formula can be referred to [28]:

$$E = E_0 + \frac{S_g E_g}{S_s}, \quad (4)$$

where E is the elastic modulus of shotcrete after conversion, GPa; E_0 is the initial elastic modulus of shotcrete, GPa; E_g is the elastic modulus of the steel arch, GPa; S_s is the equivalent replacement cross-sectional area of shotcrete, cm^2; S_g is the cross-sectional area of steel arch, cm^2.

Combined with field investigation and laboratory experiment, the physical and mechanical parameters of the surrounding rock and concrete are shown in Table 4.

4.3. Calculation Conditions. Many factors, such as terrain condition, geological condition, charging structure, detonation mode, and distance from explosive sources, can affect the strength of blasting-induced vibration [29, 30]. This study mainly selected vibration velocity peak as the analysis index of blasting-induced vibration strength. The calculation conditions comprise the combination of the 3 levels of surrounding rocks (III, IV, and V), 6 buried depths (5, 10, 20, 30, 40, 50, and 100 m), 6 net spans (1, 2, 3, 4, 5, and 6 m), and 9 different distances from explosive source (−20, −15, −10, −5, 0, 5, 10, 15, and 20 m). The blasting-induced vibration velocity peaks under different calculation conditions were calculated. The detonation mode of the right and left holes was applied initially and after the simulation process, respectively. The effects of blasting-induced vibration on the transition section of the branching-out tunnel under different conditions were discussed, and the blasting-induced vibration propagation laws in the transition section were analyzed.

4.4. Results Analysis

4.4.1. Effects of Buried Depth and Net Span. It was hypothesized in calculation that the surrounding rocks were III-level, and the bench cut method was applied. The variation curves of blasting-induced vibration velocity peak with buried depth at different net spans in the anterior tunnel are shown in Figure 6.

Figure 6 shows that the blasting-induced vibration velocity peak increases with the buried depth. The vibration velocity peak curve tends to be stable with the continuous increase in buried depth. The vibration velocity peaks of tunnels with different net spans stabilize at different buried depths. The higher the net span is, the higher the buried depth is when the vibration velocity peak stabilizes. This phenomenon can be explained as follows. When the buried depth is smaller than the net span, the coverage layer on the tunnel roof is relatively thin, and strong blasting-induced vibrations are observed, thereby weakening the vibration velocity in the anterior tunnel at the side facing the blasting. When the buried depth is higher than the net span, the coverage layer on the tunnel roof is thickened gradually, and the vibration velocity in the anterior tunnel increases

Table 4: Calculation parameters of surrounding rock and concrete.

Materials	Density (g/cm^3)	Elasticity modulus (GPa)	Poisson's ratio	Shear modulus (GPa)	Compressive strength (GPa)
III-level surrounding rock	2.5	40	0.28	18.5	0.058
IV-level surrounding rock	2.2	20	0.32	16.5	0.018
V-level surrounding rock	1.8	5	0.37	10.5	0.006
C25 concrete	2.5	40	0.18	25.0	0.145

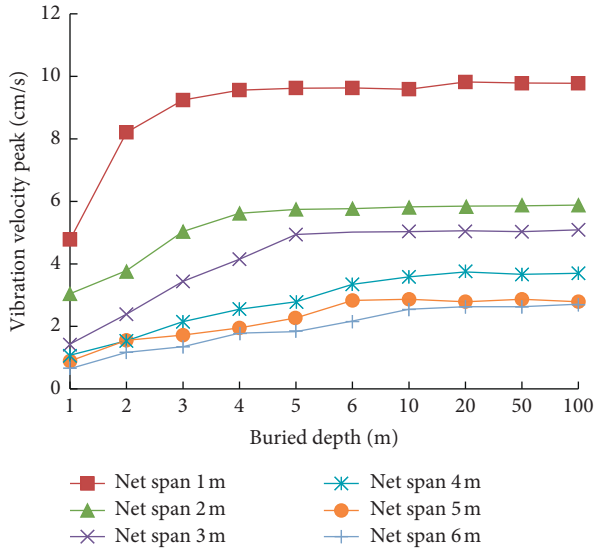

Figure 6: Variation curves of vibration velocity peak with buried depth at different net spans.

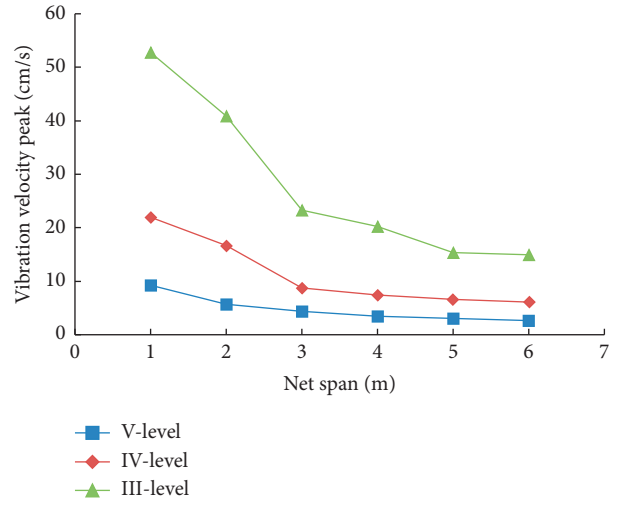

Figure 7: Variation curves of vibration velocity peak with net span under different surrounding rock levels.

accordingly. Therefore, real-time monitoring over the blasting-induced vibration velocity in the anterior tunnel and coverage layer, adjusting and optimizing the blasting design parameters, and applying surface grouting, shotcrete, and rock bolt support to the coverage layer on the roof of tunnel are suggested because the transition section of the branching-out tunnel is generally located at the tunnel portal where the buried depth is small.

4.4.2. Effects of Surrounding Rock Level and Net Span. To analyze influences of surrounding rock level and net span on the posterior tunnel, three levels of surrounding rocks (e.g., III, IV, and V) were set, and the bench cut method was used. The buried depth and net span were set as 30 m and 1–6 m, respectively. The variation curves of the blasting-induced vibration velocity peak with net span under different surrounding rock levels in the transition section are calculated (Figure 7).

Figure 7 shows that the blasting-induced vibration velocity peak in hard and integral rock mass attenuates quickly. That is, if rock masses are soft and broken, then the blasting-induced vibration velocity peak attenuates slowly. In view of net span, the relationship between blasting-induced vibration velocity peak and net span is nonlinear, because of several factors, such as surrounding rock levels. The vibration velocity peak decreases with the continuous increase in net span. When the net span is smaller than 3 m, the blasting-induced vibration velocity peak attenuates dramatically. When the net span is higher than 3 m, the blasting-induced vibration velocity peak tends to stabilize. Therefore, weak blasting under the assistance of mechanical excavation and timely support is recommended to the section with V-level surrounding rocks, net span smaller than 3 m, and poor stability. In other sections, the appropriate excavation mode shall be selected according to practical field situations and blasting-induced vibration strength, such as bench cut method, center cross diagram (CRD), or side drift method. Moreover, the blasting design scheme shall be monitored and perfected at a proper time, and blasting-induced vibration control measures shall be implemented well.

4.4.3. Effects of Excavation Methods and Net Span. Full-face excavation, upper bench, lower bench, CRD, and side drift methods were used in the calculation. The buried depth, surrounding rock level, and net span of the tunnel were set as 30 m, III-level, and 1–6 m, respectively. The variation curves of the blasting-induced vibration velocity peak with net span under different excavation methods are shown in Figure 8.

Figure 8 shows that the CRD and side drift methods, which decrease the rock mass volume and charge quantity

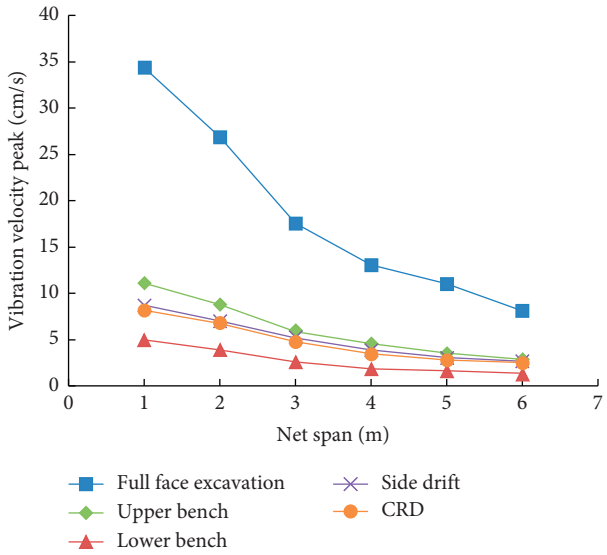

Figure 8: Variation curves of vibration velocity peak with net span under different excavation methods.

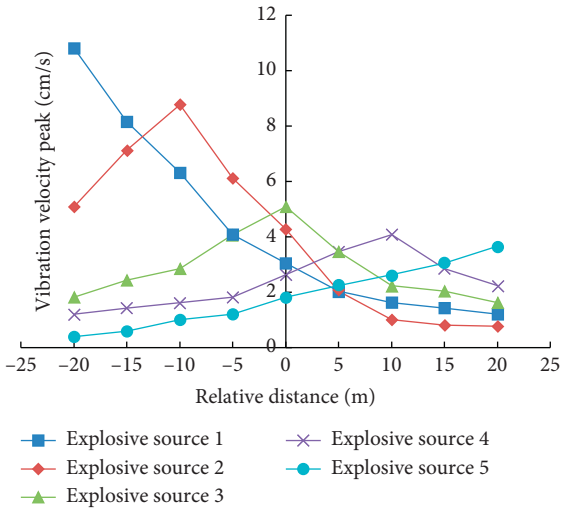

Figure 9: Variation curves of vibration velocity peak with relative distance from explosive sources.

for single-stage blasting and can reduce vibration significantly, excavate pilot tunnel first. Importantly, the pilot tunnel shall be far away from the anterior tunnel to reduce vibrations. According to the variation curve of the vibration velocity with net span, the blasting-induced vibration velocity peak curve is relatively sharp when the net span is smaller than 3 m, indicating that the reduction rate is high. When the net span is between 3 and 6 m, the curve is relatively gentle. Therefore, the use of CRD or side drift method, which has many blasting-induced vibrations to tunnels with net span smaller than 3 m, is recommended to release blasting-induced vibration waves to surrounding rocks and thereby decrease the influences of maximal segment explosive quantity on vibration of surrounding rocks. When the net span is higher than 3 m, the application of the bench cut method is suggested. The full-face excavation method is not recommended because it generates excessive blasting-induced vibration velocity.

4.4.4. Effects of Shared Rock. Suppose that the buried depth of tunnel is 30 m, and III-level surrounding rocks apply the bench cut method. The advancing directions of the tunnel, which refer to the front surface of the excavation, are 10 m and 20 m. The portal direction, which refers to the surface behind the excavation, is −10 m and −20 m. Five explosive points were set at −10, −20, 0, 10, and 20 m and were numbered as explosive sources 1–5, respectively. The variation curve of blasting-induced vibration velocity peak with distance from the explosive source is shown in Figure 9.

Figure 9 illustrates that the vibration velocity peak behind the explosive excavation surface at different explosive source points is higher than that in front of the explosive surface. The reason is related to the free face of the shared rock behind the excavation surface. At the blasting of the posterior tunnel, the free face on the shared rock behind the excavation surface can amplify the detonation wave, thereby causing the blasting-induced vibration velocity behind the excavation surface to be higher than that in front of the excavation surface. According to the blasting-induced vibration velocity peak curves, the vibration velocity peak within 10–15 m in front and behind the explosive point drops rapidly, attenuates slowly, and finally tends to stabilize. Therefore, the vibration of the surrounding rocks in the anterior tunnel within 10 m behind the explosive point is influenced to a maximum extent, thereby requiring key monitoring in construction process.

4.4.5. Effects of Anterior Tunnel Section. The calculation condition was set as V-level surrounding rock, bench cut method, 30 m buried depth, and 1–6 m net span. The side wall bottom, haunch, and spandrel at the side that faces detonation, as well as spandrel, haunch, and side wall bottom at the side behind the detonation, vault, and floor center, were chosen in the follow-up analysis. Variation curves of the blasting-induced vibration velocity peak with net span at sectional positions are shown in Figure 10.

Figure 10 shows that the blasting-induced vibration velocity peak, which is approximately 2.0–2.5 times that on the side behind the detonation at spandrel of the side facing with the detonation in the anterior tunnel, is the highest. This is because the spandrel of the side facing with the detonation is in the intersection of the shared rock and rock strata, and the explosive stress wave may generate very strong reflection effect on the interface, accompanied with superposition of reflected wave stresses. As a result, stress wave, which can amplify the blasting-induced vibration velocity on the interface, is strengthened significantly. Secondly, the blasting-induced vibration velocity peak at the haunch of the side facing with the detonation is about 6-7 times that at the side behind the detonation. The minimum blasting-induced vibration velocity peak is at the wall foot of the side behind the detonation. Generally, the blasting-induced vibration velocity at the side facing with detonation in the anterior tunnel is higher than that at the side behind

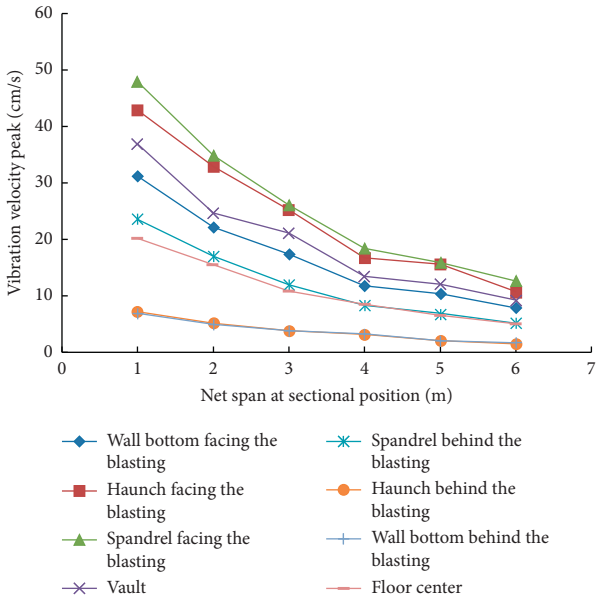

Figure 10: Variation curves of vibration velocity peak with net span at sectional positions.

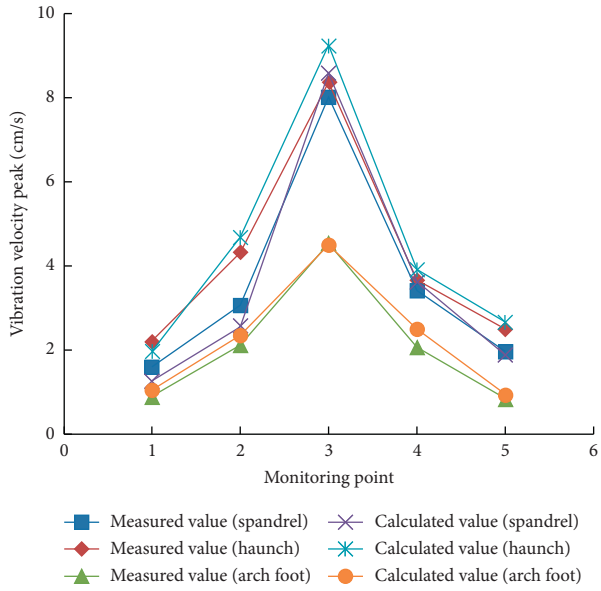

Figure 11: Variation curve of radial vibration velocity peak at different monitoring points.

detonation. According to the vibration velocity peak curve, the blasting-induced vibration velocity is negatively correlated with net span. Besides, it attenuates quickly when the net span is smaller than 4 m, but it becomes stable when the net span is higher than 4 m. Therefore, it is suggested to take spandrel and haunch at the side facing with detonation of the anterior tunnel as key points of vibration control during blasting construction of transition section of the anterior tunnel.

4.5. Comparative Analysis. The variation law of radial vibration velocity peak at spandrel, haunch, and arch foot of the side facing with detonation was concluded on the basis of the comparison between the measured results of radial vibration velocity in Table 2 and the numerical simulation results (Figure 11).

The average relative errors of the vibration speeds of the haunch, spandrel, and arch foot are 3.5%, 7.8%, and 9.8%, which are within a reasonable range based on the comparison of the measured data of each measuring point in Figure 11 with the numerical simulation calculation value, respectively. The accuracy and reliability of the numerical simulation results are verified by the measured data.

5. Blasting-Induced Vibration Control Measures

(1) Selection of tunnel excavation method: the transition section of a branching-out tunnel has characteristics of small buried depth, short net span, complicated structure, and poor stability. Long pipe-roof protection shall be applied for advanced support before the excavation. CRD or side drift method is recommended. The footage driving cycle is controlled within 0.5–1.5 m, and the "new Austrian tunneling method" shall be adopted for supporting in time.

(2) Controlling maximal segment explosive quantity and choosing reasonable cut blasting mode: according to Sodev's empirical formula, the maximal segment explosive quantity is proportional to blasting-induced vibration velocity. Therefore, decreasing the maximal segment explosive quantity is a major method of controlling the blasting-induced vibration velocity. The double wedge-shaped cut blasting was chosen combined with practical situations of this project. The big wedge-shaped cut-hole was changed into second-level small wedge-shaped cut-hole. This not only can decrease segment explosive quantity of small wedge-shaped cut-hole but also can weaken the clamping effect of the first-level cut-hole explosion, thus enabling it to control blasting-induced vibration and improve the cut-hole explosion effect.

(3) Selection of explosion interval and number of detonator segments: according to feedback data and timely adjusted explosion interval, weakening interference effect during explosion and avoiding superposition of explosive blasting waves decrease the blasting-induced vibration velocity peak significantly. During the construction, nine segments of detonators were set at the upper left of the posterior tunnel and the detonation interval was set 50–140 ms. In particular, it applied floor blast-hole staged detonation, which was proven effective in reducing vibration.

(4) Geological condition and distance from explosive sources: vibration strength is related to blasting-induced vibration propagation media. Near the explosive source, the blasting-induced vibration velocity decreased continuously with the increase in distance. Therefore, sections which have poor geological conditions and

short distances between explosive excavation surface and the supporting structure shall be the key area of vibration control. It is recommended to choose the appropriate blasting scheme.

6. Conclusions

This paper mainly aims to study the influences of blasting excavation in posterior tunnel of the transition section on supporting structures of the anterior tunnel. Based on the field blasting-induced vibration monitoring datum and numerical simulation presented in this study, the following conclusions can be drawn:

(1) Influenced by posterior tunnel blasting, the blasting-induced vibration velocity peak of shared rock in the anterior tunnel attenuates regularly along the advancing direction. The blasting-induced vibration velocity peak behind the blasting excavation surface is higher than that in front of the blasting excavating surface. The region within 10 m behind the blasting excavation surface is the key position of blasting-induced vibration control in the transition section of a branching-out tunnel.

(2) CRD or side drift method is recommended for IV-level, V-level, and III-level surrounding rocks with net span smaller than 3 m in the transition section of a branching-out tunnel. However, the bench cut method is chosen for III-level surrounding rocks with net span higher than 3 m. The full-face excavation method is not recommended in the transition section. V-level surrounding rocks have soft and broken rock strata, so weak or loose blasting shall be applied under the assistance of mechanical excavation.

(3) The blasting-induced vibration velocity peak at the spandrel and haunch of the side facing with the detonation in the anterior tunnel is the highest at 2.0–2.5 and 6-7 times those at the spandrel and haunch behind the detonation, respectively. Therefore, these two sections are key positions to control blasting-induced vibration velocity.

(4) The propagation laws of blasting-induced vibration wave are related to the surrounding rock condition, buried depth, construction method, and net span in the tunnel. The numerical simulation results further optimize the blasting scheme. The maximum vibration velocity in monitoring is 8.35 cm/s, proving that the double wedge-shaped cut blasting and the floor blast-hole staged detonation can control vibration velocity effectively.

Data Availability

The data sets used to support the findings of this study are included within the article.

Conflicts of Interest

The authors declare that they have no conflicts of interest.

Acknowledgments

This work was supported by the National Natural Science Foundation of China (no. 51608183), the China Scholarship Council (no. 201808430341), and the Natural Science Foundation of Hunan Province in China (no. 2018JJ3022).

References

[1] S. Song, S. Li, L. Li et al., "Model test study on vibration blasting of large cross-section tunnel with small clearance in horizontal stratified surrounding rock," *Tunnelling and Underground Space Technology*, vol. 92, p. 103013, 2019.

[2] T.-H. Ling, F. Cao, S. Zhang, L. Zhang, and D.-P. Gu, "Blast vibration characteristics of transition segment of a branch tunnel," *Journal of Vibration and Shock*, vol. 37, no. 2, pp. 43–50, 2018.

[3] L.-Y. Yu, S.-C. Li, X.-H. Guo, and S.-B. Shi, "Study of stability of transition segment for bifurcation tunnel," *China Journal of Highway and Transport*, vol. 24, no. 1, pp. 89–95, 2011.

[4] F. Cao, T.-H. Ling, J.-S. Liu, L. Zhang, and D.-P. Gu, "Analysis on blasting vibration effect of shallow multi-arch section of bifurcated tunnel," *Journal of Highway and Transportation Research and Development*, vol. 35, no. 2, pp. 86–94, 2018.

[5] J. Wang, S. Tang, H. Zheng, C. Zhou, and M. Zhu, "Flexural behavior of a 30-meter full-scale simply supported prestressed concrete box girder," *Applied Sciences*, vol. 10, no. 9, p. 3076, 2020.

[6] A. Li, D.-L. Zhang, Q. Fang, J.-W. Luo, L.-Q. Cao, and Z.-Y. Sun, "Safety distance of shotcrete subjected to blasting vibration in large-span high-speed railway tunnels," *Shock And Vibration*, vol. 2019, Article ID 2429713, 14 pages, 2019.

[7] Y. Xia, N. Jiang, C. Zhou, and X. Luo, "Safety assessment of upper water pipeline under the blasting vibration induced by Subway tunnel excavation," *Engineering Failure Analysis*, vol. 104, pp. 626–642, 2019.

[8] S.-C. Li, H.-P. Wang, and X.-F. Zheng, "Forked tunnel stability analysis and its construction optimization research," *Chinese Journal of Rock Mechanics and Engineering*, vol. 27, no. 3, pp. 447–457, 2008.

[9] X.-W. Chai, S.-S. Shi, Y.-F. Yan, J.-G. Li, and L. Zhang, "Key blasting parameters for deep-hole excavation in an underground tunnel of phosphorite mine," *Advances in Civil Engineering*, vol. 2019, Article ID 4924382, 9 pages, 2019.

[10] J. Yang, J. Cai, C. Yao, P. Li, Q. Jiang, and C. Zhou, "Comparative study of tunnel blast-induced vibration on tunnel surfaces and inside surrounding rock," *Rock Mechanics and Rock Engineering*, vol. 52, no. 11, pp. 4747–4761, 2019.

[11] S. Zhang, W.-C. He, Y.-S. Li, D. Hu, and X. Cai, "Research on identification of tunnel cavity fillings by time-energy density analysis based on wavelet transform," *Journal of China Coal Society*, vol. 44, no. 11, pp. 3504–3514, 2019.

[12] A. Sharafat, W. A. Tanoli, G. Raptis, and J. W. Seo, "Controlled blasting in underground construction: a case study of a tunnel plug demolition in the Neelum Jhelum hydroelectric project," *Tunnelling and Underground Space Technology*, vol. 93, p. 103098, 2019.

[13] J. Chen, H. Yu, A. Bobet, and Y. Yuan, "Shaking table tests of transition tunnel connecting TBM and drill-and-blast

tunnels," *Tunnelling and Underground Space Technology*, vol. 96, p. 103197, 2020.

[14] N. Jiang, C.-B. Zhou, X.-D. Luo, and S.-W. Lu, "Damage characteristics of surrounding rock subjected to VCR mining blasting shock," *Shock and Vibration*, vol. 2015, Article ID 373021, 8 pages, 2015.

[15] K. Xu, Q. Deng, L. Cai, S. Ho, and G. Song, "Damage detection of a concrete column subject to blast loads using embedded piezoceramic transducers," *Sensors*, vol. 18, no. 5, p. 1377, 2018.

[16] J. Yang, W. Lu, M. Chen, P. Yan, and C. Zhou, "Microseism induced by transient release of in situ stress during deep rock mass excavation by blasting," *Rock Mechanics and Rock Engineering*, vol. 46, no. 4, pp. 859–875, 2012.

[17] X. Tian, Z. Song, and J. Wang, "Study on the propagation law of tunnel blasting vibration in stratum and blasting vibration reduction technology," *Soil Dynamics and Earthquake Engineering*, vol. 126, p. 105813, 2019.

[18] Z. Hu, K. Du, J.-X. Lai, and Y.-L. Xie, "Statistical analysis of influence of cover depth on loess tunnel deformation in NW China," *Advances in Civil Engineering*, vol. 2019, Article ID 2706976, 12 pages, 2019.

[19] H.-B. Zhao, Y. Long, X.-H. Li, and L. Lu, "Experimental and numerical investigation of the effect of blast-induced vibration from adjacent tunnel on existing tunnel," *KSCE Journal of Civil Engineering*, vol. 20, no. 1, pp. 431–439, 2015.

[20] S. Zhang, Z.-D. Wang, Y.-S. Li, G.-H. Fu, and Z.-B. Liu, "Characteristics analysis of blast vibration signals based on pattern adapted continuous wavelet energy spectrum," *Blasting*, vol. 36, no. 2, pp. 105–110, 2019.

[21] GB 6722-2014, *Safety Regulations for Blasting*, China Society of Engineering Blasting, Standards Press of China, Beijing, China, 2014.

[22] W.-B. Lu, Y. Luo, M. Chen, and D.-Q. Shu, "An introduction to Chinese safety regulations for blasting vibration," *Environmental Earth Sciences*, vol. 67, no. 7, pp. 1951–1959, 2012.

[23] X. Liu, Q. Fang, and D. Zhang, "Mechanical responses of existing tunnel due to new tunnelling below without clearance," *Tunnelling and Underground Space Technology*, vol. 80, pp. 44–52, 2018.

[24] M. Yin, H. Jiang, Y. Jiang, Z. Sun, and Q. Wu, "Effect of the excavation clearance of an under-crossing shield tunnel on existing shield tunnels," *Tunnelling and Underground Space Technology*, vol. 78, pp. 245–258, 2018.

[25] C.-M. Lin, Z.-C. Zhang, Q. Zheng, H.-L. Zheng, and M. Li, "Study on the soft surrounding rocks stability and supporting parameters of two-to-fourlane tunnel of small clear-distance by CD method," *China Civil Engineering Journal*, vol. 46, no. 7, pp. 124–132, 2013.

[26] Z.-G. Zhu, M.-L. Shu, Y.-Q. Zhu, and X.-L. Sun, "Field monitoring on blasting vibration and dynamic response of ultra-small spacing tunnels," *Rock and Soil Mechanics*, vol. 33, no. 12, pp. 3747–3752, 2012.

[27] W.-P. Wu, X.-T. Feng, C.-Q. Zhang, S.-L. Qiu, and Z.-H. Li, "Reinforcing mechanism and simulating method for reinforcing effects of systemically grouted bolts in deep-buried hard rock tunnels," *Chinese Journal of Rock Mechanics and Engineering*, vol. 31, no. 1, pp. 2711–2721, 2012.

[28] S.-C. Li, W.-S. Zhu, W.-Z. Chen, and S.-C. Li, "Application of elasto-plastic large displacement finite element method to the study of deformation prediction of soft rock tunnel," *Chinese Journal of Rock Mechanics and Engineering*, vol. 21, no. 4, pp. 466–470, 2002.

[29] G.-S. Zhong, L.-P. Ao, and K. Zhao, "Influence of explosion parameters on wavelet packet frequency band energy distribution of blast vibration," *Journal of Central South University*, vol. 19, no. 9, pp. 2674–2680, 2012.

[30] Z. Zhang, C.-B. Zhou, S.-W. Lu, C. Wu, and C. Wang, "Propagation characteristics of ground vibration induced by subsurface blasting excavation in an ultra-shallow buried underpass," *Journal of Central South University (Science and Technology)*, vol. 48, no. 8, pp. 2119–2125, 2017.